MEMS TECHNOLOGIES IN LIFE SCIENCES

H.P. Lang[1], F. Huber[1], J. Zhang[1], and Ch. Gerber[1]
[1]Swiss Nano Institute, University of Basel, Klingelbergstrasse 82, 4056 Basel, SWITZERLAND

ABSTRACT

MEMS technologies have come of age. They are ubiquitous in many applications in life sciences and have entered the clinic. Micro-fabricated silicon cantilevers arrays offer a novel label-free approach where ligand-receptor binding interactions occurring on the sensor generate nanomechanical signals like bending or a change in mass, which is optically detected in-situ. It enables the detection of multiple unlabeled biomolecules simultaneously down to picomolar concentrations within minutes in differential measurements including reference cantilevers on arrays of eight sensors. Further applications include monitoring of gene expression in interferon treatment and efficacy testing in melanoma cancer treatment based on total RNA samples.

KEYWORDS

Cantilever sensors, melanoma, DNA, surface stress, microcantilever array

INTRODUCTION

Microfabricated silicon cantilever sensor arrays represent a powerful platform for a broad range of detection applications in physics [1], chemistry [2], material science [3], biology [4] and medicine [5]. This label-free, real-time technology makes it possible to monitor the interactions of a wide range of molecules, including proteins [6] and nucleic acids [7]. The sensor response is mechanical bending due to absorption of molecules on the cantilever surface.

EXPERIMENTAL

All experiments were performed using commercially available static mode cantilever arrays with eight identical silicon cantilevers having the following dimensions: 500µm in length, 100µm in width, and 0.9µm in thickness (IBM Research GmbH, Rüschlikon, Switzerland).

The preparation of cantilever sensor arrays has been described previously [8]. Prior to use, cantilever arrays undergo the following procedure: cleaned twice in freshly prepared Piranha solution (H_2O_2:H_2SO_4=1:1) for 30 min, rinsed with Nanopure water and absolute ethanol, dried on a hot plate at 75°C. To prevent non-specific binding on the bottom side of the cantilever, the array was immersed into a 10 mM ethanolic solution of 2-[methoxy(polyethyleneoxy)propyl]trimethoxysilane for 45min, washed three times using absolute ethanol and dried with argon. Then a 2nm thick titanium layer and a 20nm thick gold layer were deposited onto the top side of the cantilever using an electron beam evaporator (EVA300, Alliance Concept, Cran Gevrier, France). Each of the freshly prepared gold-coated cantilever arrays was functionalized with thiolated oligonucleotide probes for target capture and thiolated reference oligonucleotides, respectively. The functionalized array was rinsed using 10 mM PBS buffer and stored at +4°C.

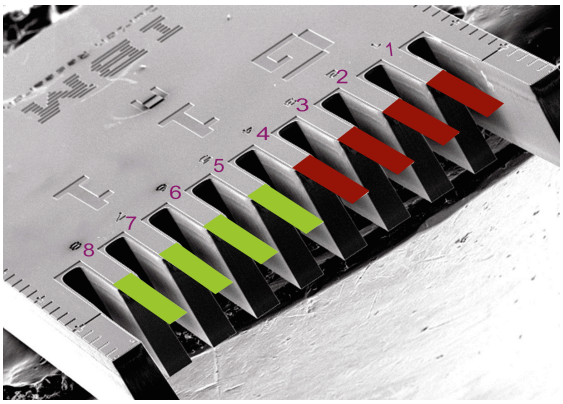

Figure 1: Scanning electron micrograph of an array of eight microcantilevers (length 500µm, width 100µm, thickness 0.9 µm). Different functionalization of sensor and reference cantilevers is schematically indicated by coloring individual cantilevers in red and green.

RESULTS AND DISCUSSION

Here we present three selected examples of applications of microcantilever sensors.

Optimization of DNA hybridization efficiency by pH-driven nanomechanical bending

The accessibility and binding affinity of DNA are two key parameters that affect hybridization efficiency in surface-based biosensor technologies. Greater accessibility will ultimately result in higher hybridization efficiency. Here, we utilized microcantilevers functionalized with single-strand DNA to increase hybridization efficiency and accessibility of surface-bound oligonucleotides to the complementary target DNA without need of formation of mixed ssDNA and mercaptohexanol monolayers or other modifications, as reported by others [9, 10]. The extreme sensitivity of cantilever sensors to variations in environmental pH due to pH-induced conformational changes is a major advantage, allowing rapid nanomechanical responses of ssDNA functionalized microcantilevers.

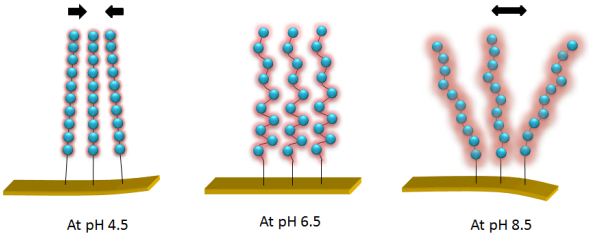

Figure 2: Schematic of single stranded DNA immobilized of a cantilever in different pH environments. Black double arrows indicate interaction forces.

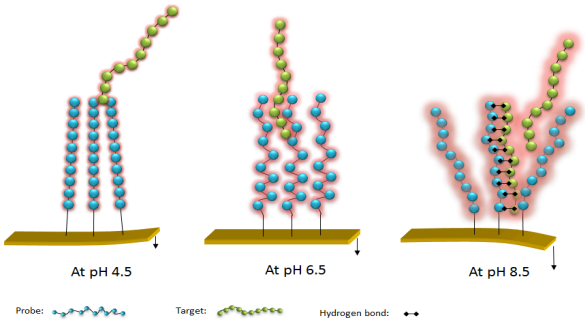

Figure 3: pH-induced surface hybridization affinity depends on conformational changes of ssDNA chains. ssDNA molecules are shown in the target complementary strands in red. At low pH 4.5 an attractive electrostatic force due to partial protonation acts on ssDNA strands. The beginning of deprotonation sets in at neutral pH 6.5 beyond the isoelectric point. At high pH 8.5 ssDNA strands are fully deprotonated and the separation between strands increases due to electrostatic repulsion forces.

At low pH 4.5 the accessibility of ssDNA chains is low resulting in low hybridization efficiency, as attractive forces dominate the force between neighboring ssDNA probes, leading to a tensile surface stress and implying reduced accessibility of bound ssDNA probe for hybridization to complementary strands. At neutral pH 6.5 the ssDNA strands are more accessible to their complements yielding a higher hybridization efficiency. In contrast, at high pH 8.5, the steric interaction between neighboring ssDNA strands is decreased by higher electrostatic repulsive forces, which bend the microcantilever away from the gold surface providing more space for target DNA, resulting in low steric hindrance and hence high hybridization efficiency (Figures 2 and 3).

Testing the nanomechanical cantilever bending response on hybridization at different pH reveals an optimized environmental condition of pH 7.5-8.5, as illustrated in Figure 4.

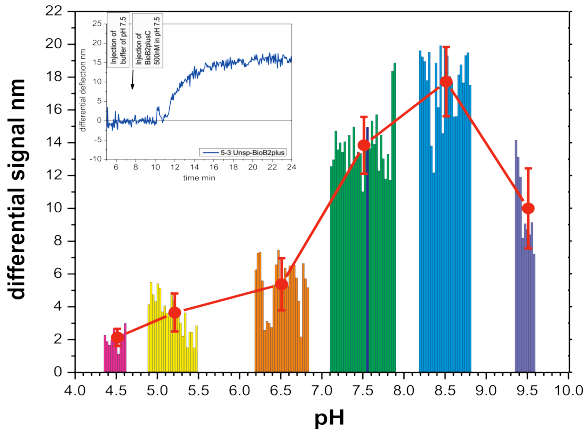

Figure 4: Each bar represents an independent measurement of the difference of responses of a sensor and a reference cantilever (see inset showing the response represented by the bar displayed in dark blue). Measurements were performed on 10 different arrays to increase statistics.

The average of responses at a particular pH value is marked by a red dot and a standard deviation error bar. As the differential nanomechanical response is a measure for hybridization efficiency, we identify an optimized range for hybridization efficiency between 7.5 and 8.5, corresponding to physiological conditions.

Cantilever deflection scales with pH-dependent surface hybridization efficiency due to high target DNA accessibility. Hence by changing pH, hybridization efficiency is adjusted. In addition, the observation of pH-dependent surface hybridization on microcantilevers has proved that the accessibility and affinity of target molecules is governed by the interaction force and steric hindrance between the neighboring ssDNA strands on the microcantilever surface. Our findings reveal that pH plays a major role in the generation of nanomechanical surface stress of hybridization.

Experiments have been performed repeatedly and reprocucibly with high accuracy, as shown in Figures 4 and 5.

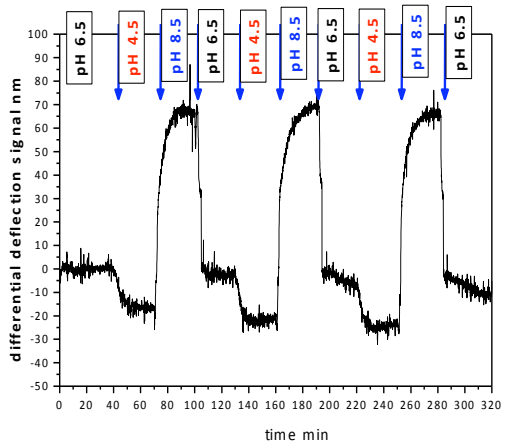

Figure 5: Serial differential deflection measurements (sensor minus reference) to demonstrate robustness and reproducibility.

An optimized pH range for hybridization can be used for improving the sensitivity of DNA-based microcantilever array sensors to increase accessibility and affinity of ssDNA to their complements during hybridization and to provide detailed information on the fundamental understanding of the role of surface stress. Selecting the pH value during surface hybridization allows to maximize hybridization efficiency [11].

Direct detection of a BRAF mutation in total RNA from melanoma cells using cantilever arrays

Malignant melanoma, the deadliest form of skin cancer, is characterized by a predominant mutation in the BRAF gene [12]. Drugs that target tumours carrying this mutation have recently entered the clinic [13]. Accordingly, patients are routinely screened for mutations in this gene to determine whether they can benefit from this type of treatment, as only about 50% of patients carry this mutation. The current gold standard for mutation screening uses real-time polymerase chain reaction and

sequencing methods. Here we show that an assay based on microcantilever arrays can detect the mutation nanomechanically without amplification in total RNA samples isolated from melanoma cells. The assay is based on a BRAF-specific oligonucleotide probe. We detected mutant BRAF at a concentration of 500 pM in a 50-fold excess of the wild-type sequence. The method was able to distinguish melanoma cells carrying the mutation from wild-type cells using as little as 20 ng/µL of RNA material, without prior PCR amplification and use of labels [14].

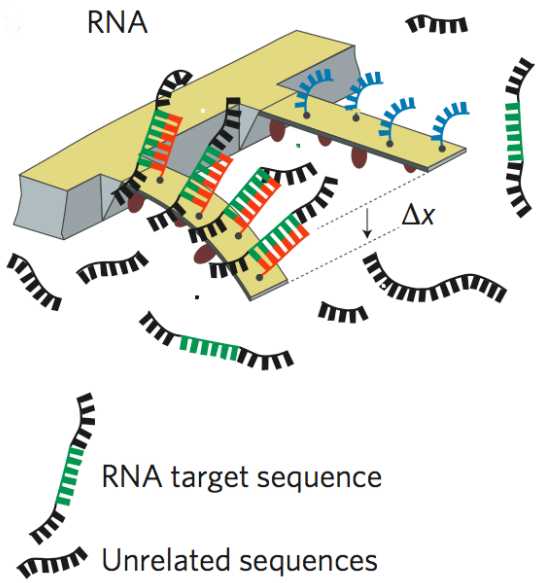

Figure 6: Binding of the complementary (matching) sequence (depicted in green) to the probe oligonucleotide (red) produces bending of the probe cantilever, giving rise to a differential deflection Δx. No binding occurs on the reference cantilever.

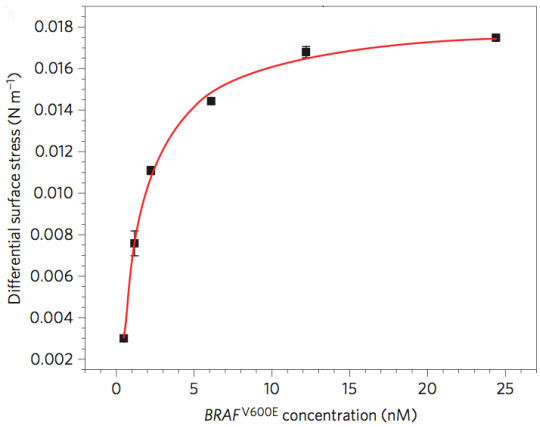

Figure 7: Langmuir plot of compressive surface stress from hybridization experiments for different concentrations of mutant DNA in background wild-type DNA

In a first set of experiments we assessed the specificity of the BRAF mutation using some cantilevers in an array functionalized with an oligonucleotide carrying the mutation and others with a unrelated reference oligonucleotide (Fig. 6). The sensing cantilever responded only to the mutated sequence and not to the wildtype sequence. The corresponding concentration dependence is shown in Fig. 7. The fit from the Langmuir plot yields a change of Gibbs free energy of -49.8 kJ/mol and is in good agreement with results obtained by surface plasmon resonance and theoretical calculations.

.

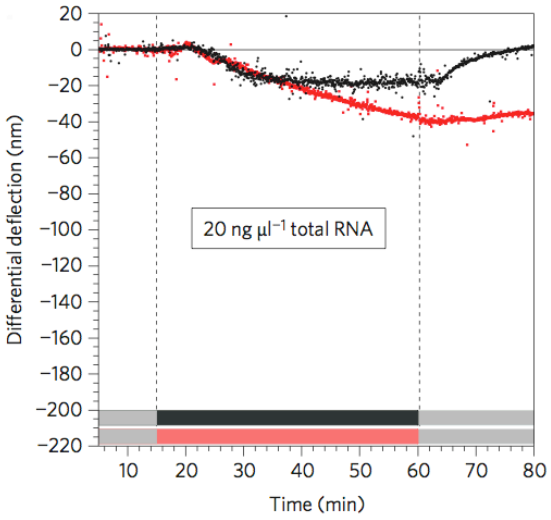

Figure 8: Detection of mutated versus wild-type (black curve) and mutated (red curve) BRAF in total RNA samples showing a response difference of about 20 nm in deflection. The dark gray and light red bars represent injection of wild type and mutated RNA from cells in buffer, the light gray bar stands for buffer injection.

In a second step we utilized messenger RNA from melanoma cells for a direct measurement of the mutation with our label-free and amplification-free cantilever sensing technique. Four concentrations in the range 5 - 300 ng/µL were measured, suggesting a lower limit of detection between 5 and 20 ng/µL total RNA (Fig. 8). Such concentrations are comparable to those present in patient biopsies, allowing applicability of the technique in clinic. Although we have focused here on the detection of BRAF V600E mutations in melanoma, the microcantilever approach can be extended to other relevant mutations recurring in other types of cancer, such as gastrointestinal tumors and lung cancer. Due to the parallel format of the assay, the presence of multiple mutations may be interrogated simultaneously, allowing a more detailed prognosis, facilitating fast and personalized medical diagnostics.

Antibody recognition of tumor cells on the cantilever surface

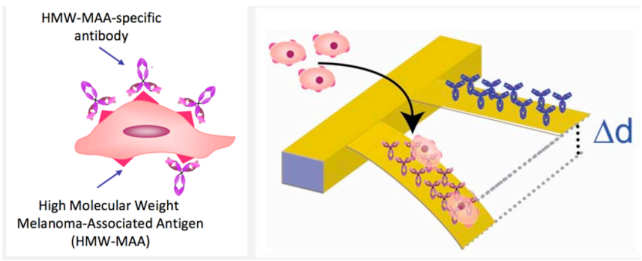

Figure 9: Binding of melanoma cells to specific antibodies on the cantilever produces bending.

To directly capture circulating tumor cells (Fig. 9), we developed a protocol for binding melanoma cells on a cantilever functionalized with high molecular weight melanoma associated antibody (HMW-MAA).

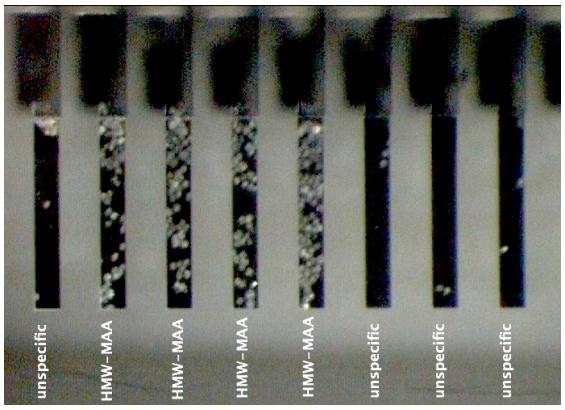

Figure 10: Melanoma cells stick even after thorough washing with buffer only on HMW-MAA functionalized cantilevers, but not on cantilevers coated with an unspecific antibody. Such specific adhesion allows to capture melanoma cells for further analysis on the cantilever.

The cell adhesion process has been followed both with optical microscopy (Fig. 10) and in our cantilever array sensor setup monitoring cantilever deflections, whereby specific melanoma cell adhesion produced a large differential deflection signal of about 2 μm.

The cantilever sensor method has the following advantages: 1. no labeling or pre-amplification by PCR necessary, 2. cost-efficient, 3. due to the array format, the analysis can be paralleled, so that different markers or mutations can be simultanelously interrogated. Nanomechanical cantilever array sensors represent an excellent example demonstrating how medical diagnosis can benefit from an interdisciplinary approach.

ACKNOWLEDGEMENTS

We acknowledge ongoing support from Michel Despont and Ute Drechsler (IBM Research GmbH, Rüschlikon, Switzerland) for providing cantilever arrays. We thank the National Center of Competence for Nanoscale Science (NCCR Nano), the Swiss Nano Institute (SNI), the NanoTera program, the Cleven foundation and the Swiss National Science Foundation for financial support.

REFERENCES

[1] M.K. Ghatkesar, E. Rakhmatullina, H.P. Lang, Ch. Gerber, M. Hegner, T. Braun. "Multi-parameter microcantilever sensor for comprehensive characterization of newtonian fluids". *Sensors Actuators B*, vol. 135, 133-138 (2008).

[2] Y. Dong, G. Wei, Q. Zhou, Y. Zheng, Z. You. "Characterization of the gas sensors based on polymer-coated resonant microcantilevers for the detection of volatile organic compounds". *Anal. Chim. Acta*, vol. 671, 85–91 (2010).

[3] M. Toda, A.N. Itakura, S. Igarashi, K. Büscher, J.S. Gutmann, K. Graf, R. Berger. "Surface Stress, thickness, and Mass of the First Few Layers of Polyelectrolyte". *Langmuir,* vol. 24, 3191-3198 (2008).

[4] M.P. Stewart, Y. Toyoda, A.A. Hyman, D.J. Muller, "Force probing cell shape changes to molecular resolution". *Trends in Cell Biology*, vol. 36, 444-450 (2011).

[5] J.W. Ndieyira, M. Watari, A.D. Barrera, D. Zhou, M. Vogtli, M. Batchelor, M. Cooper, T. Strunz, M.A. Horton, C. Abell, T. Rayment, G. Aeppli, R.A. McKendry,. "Nanomechanical detection of antibiotic mucopeptide binding in a model for superbug drug resistance". *Nat. Nanotechnol.,* vol. 3, 691 – 696 (2008).

[6] N. Backmann, C. Zahnd, F. Huber, A. Bietsch, A.; Plückthun, H.P. Lang, H.-J. Güntherodt, M. Hegner, Ch. Gerber. "A label-free immunosensor array using single-chain antibody fragments", *Proc. Natl. Acad. Sci. U.S.A*., vol 102, 14587-14592 (2005).

[7] J. Zhang, H.P. Lang, F. Huber, A. Bietsch, W. Grange, U. Certa, R.A. McKendry, H.-J. Guntherodt, M. Hegner, Ch. Gerber. "Rapid and label-free nanomechanical detection of biomarker transcripts in human RNA". *Nat. Nanotechnol*., vol 1, 214-220 (2006).

[8] R.A. McKendry, J. Zhang, Y. Arntz, T. Strunz, M. Hegner, H.P. Lang, M.K. Baller, U. Certa, E. Meyer, H.-J. Güntherodt, Ch. Gerber. "Multiple label-free biodetection and quantitative DNA binding assays on a nanomechanical cantilever array". *Proc. Natl. Acad. Sci. U.S.A.,* vol. 99, 9783-9788 (2002).

[9] M.S. Shchepinov, C. Case-Green, E.M. Southern, "Steric factors influencing hybridisation of nucleic acids to oligonucleotide arrays", *Nucl. Acids Res.* vol. 25, 1155 (1997).

[10] S. Peeters, T. Stakenborg, G. Reekmans, W. Laureyn, L. Lagae, A. Van Aerschot, "Impact of spacers on the hybridization efficiency of mixed self-assembled DNA/alkanethiol films", *Biosens. Bioelectron.* vol. 24, 72 (2008).

[11] J. Zhang, H.P. Lang, G. Yoshikawa, Ch. Gerber., "Optimization of DNA hybridization efficiency by pH-driven nanomechanical bending". *Langmuir* vol. 28, 6494-6501 (2012).

[12] R. Roskoski, "RAF protein-serine/threonine kinases: structure and regulation". *Biophys. Res. Commun.* vol. 399, 313 (2010).

[13] H. Halait et al., "Analytical performance of a real-time PCR-based assay for V600 mutations in the BRAF gene, used as the companion diagnostic test for the novel BRAF inhibitor Vemurafenib in metastatic melanoma", *Diagn. Mol. Pathol. vol.* 21, 1 (2012).

[14] F. Huber, H.P. Lang, N. Backmann, D. Rimoldi, Ch. Gerber, "Direct detection of a BRAF mutation in total RNA from melanoma cells using cantilever arrays", *Nat. Nanotechnol*. vol. 8, 125–129 (2013).

CONTACT

*Ch. Gerber, tel: +41 79 614 94 09;
Christoph.Gerber@unibas.ch